



# eVe Lidar Measurements during the ASKOS/JATAC Campaign <sup>†</sup>

Peristera Paschou <sup>1,2,\*</sup> , Nikolaos Siomos <sup>3</sup>, Eleni Marinou <sup>1</sup> , Samira Moussa Idrissa <sup>4</sup>, Daniel Tetteh Quaye <sup>4</sup>, Dêgbé Désiré Fiogbe Attannon <sup>4</sup>, Charoula Meleti <sup>2</sup>, Jonas von Bismarck <sup>5</sup>, Thorsten Fehr <sup>6</sup> and Vassilis Amiridis <sup>1</sup>

- <sup>1</sup> Institute of Astronomy, Astrophysics, Space Applications and Remote Sensing (IASSARS), National Observatory of Athens, 15236 Athens, Greece; elmarinou@noa.gr (E.M.); vamoir@noa.gr (V.A.)  
<sup>2</sup> Laboratory of Atmospheric Physics, Physics Department, Aristotle University of Thessaloniki, 54124 Thessaloniki, Greece; meleti@auth.gr  
<sup>3</sup> Meteorological Institute, Ludwig Maximilian University of Munich, 80539 Munich, Germany; nikolaos.siomos@physik.uni-muenchen.de  
<sup>4</sup> West African Science Service Centre on Climate Change and Adapted Land Use (WASCAL), Atlantic Technical University, Sao Vicente C.P. 163, Cape Verde; sidrissa@uta.cv (S.M.I.); dquaye@uta.cv (D.T.Q.); dattannon@uta.cv (D.D.F.A.)  
<sup>5</sup> European Space Agency Centre for Earth Observation (ESA/ESRIN), 00044 Frascati, Italy; jonas.von.bismarck@esa.int  
<sup>6</sup> European Space Agency European Space Research and Technology (ESA/ESTEC), 2201 AZ Noordwijk, The Netherlands; thorsten.fehr@esa.int  
\* Correspondence: pepaschou@noa.gr  
<sup>†</sup> Presented at the 16th International Conference on Meteorology, Climatology and Atmospheric Physics—COMECAP 2023, Athens, Greece, 25–29 September 2023.

**Abstract:** The eVe lidar is a scanning system that can perform combined linear/circular polarization and Raman measurements at 355 nm and consists of the European Space Agency's (ESA) reference aerosol lidar system. eVe was deployed in the ASKOS campaign, which was held in Cabo Verde during the summer/autumn of 2021 and 2022, for the validation of the aerosol products of the ESA's Aeolus mission. During the campaign, eVe performed routine linear/circular depolarization measurements during Aeolus overpasses as well as dual-field-of-view measurements for the investigation of multiple scattering effects on dust layers. Herein, we present an overview of the acquired measurements and findings.

**Keywords:** eVe lidar; linear polarization; circular polarization; ASKOS; JATAC; Aeolus reference lidar; Aeolus aerosol cal/val



**Citation:** Paschou, P.; Siomos, N.; Marinou, E.; Idrissa, S.M.; Quaye, D.T.; Attannon, D.D.F.; Meleti, C.; von Bismarck, J.; Fehr, T.; Amiridis, V. eVe Lidar Measurements during the ASKOS/JATAC Campaign. *Environ. Sci. Proc.* **2023**, *26*, 168. <https://doi.org/10.3390/environsciproc2023026168>

Academic Editors: Konstantinos Moustiris and Panagiotis Nastos

Published: 5 September 2023



**Copyright:** © 2023 by the authors. Licensee MDPI, Basel, Switzerland. This article is an open access article distributed under the terms and conditions of the Creative Commons Attribution (CC BY) license (<https://creativecommons.org/licenses/by/4.0/>).

## 1. Introduction

The Aeolus mission is an Earth Explorer Core mission of the European Space Agency (ESA) [1,2], which provides for the first time vertically resolved wind and aerosol measurements from an HSRL lidar in the troposphere and lower stratosphere on a global scale [3,4]. Aeolus was launched in August 2018, and dedicated experimental campaigns have been implemented for the calibration and validation of its products. To this end, the Joint Aeolus Tropical Atlantic Campaign (JATAC) has been implemented in the Cabo Verde islands during 2021 and 2022 with the main aim of collecting quality-assured reference measurements for the calibration and validation of Aeolus products in intense dust loads and in the tropics [5]. In ASKOS, which is the ground-based component of JATAC, a suite of remote sensing and in situ instrumentation has been utilized to collect wind, aerosol, and cloud observations of high quality [6]. eVe lidar, the ESA's novel ground reference system, was deployed in ASKOS and provided reference linear and circular depolarization measurements for the validation of the aerosol properties from Aeolus. Additionally, dual-field-of-view measurements of clouds and dust layers were performed for the investigation

of particles multiple scattering effects. Herein, an overview of the acquired measurements and the first findings are presented.

## 2. Materials and Methods

### 2.1. The ASKOS Campaign

In the framework of JATAC, the ASKOS experiment was held at the Ocean Science Center of Mindelo (OSCM) on the island of São Vicente in Cabo Verde and implemented in two phases (Phase I: July/September 2021; Phase II: June/September 2022). For the ASKOS operations, a remote sensing facility for wind, aerosols, and clouds was set up, comprising active and passive remote sensors. The instrumentation includes a PollyXT multiwavelength Raman-polarization lidar, a sun-photometer, a scanning Doppler wind lidar (HALO), a microwave radiometer, and a W-band doppler cloud radar. Next to these aerosol, cloud, and wind remote sensing facilities, additional instrumentation has been deployed, such as the eVe lidar for the validation of the Aeolus Level 2A (L2A) products, the Wall-e lidar along with a solar polarimeter for providing measurements of particle orientation, the meteorological radiosondes for acquiring profiles of the atmospheric parameters, and the atmospheric electricity when accompanied with tethered electricity sensors. To complement the above observations with radiation measurements, an actinometric platform and a net radiation instrument were installed at the operations site. Last but not least, the ASKOS dataset was enriched by in situ measurements onboard unmanned aerial vehicles (UAVs) for aerosol characterization.

### 2.2. The eVe Lidar

The eVe lidar is a combined linear/circular polarization lidar system with Raman capabilities that operates at 355 nm. A detailed description of the lidar system can be found in [7]. In brief, the lidar is designed to be a mobile and flexible system, and it is implemented in a dual-laser/dual-telescope configuration that can point at multiple azimuth and off-zenith angles. This configuration allows eVe to simultaneously reproduce the operation and the pointing geometry of any lidar (spaceborne or ground-based) that emits linearly or circularly polarized light, such as the Atmospheric Laser Doppler Instrument (ALADIN) onboard Aeolus. The eVe lidar products are the vertical profiles of the particle backscatter and extinction coefficients and lidar ratio retrieved using the linear and circular emission, the volume and particle linear depolarization ratios, and the volume and particle circular depolarization ratios at 355 nm. Additionally, eVe is capable of directly retrieving the Aeolus-like backscatter coefficient and Aeolus-like lidar ratio profiles for the validation of the corresponding Aeolus L2A products. The Aeolus-like profiles are the ground-based lidar products harmonized with the Aeolus Level 2A products while considering the misdetection of the cross-polar component of the backscattered light from Aeolus (for more details, see Appendix A of [7]).

The acquired eVe dataset during ASKOS includes testing and routine measurements at multiple pointing angles (vertical and off-zenith) during daytime and nighttime. The majority of the routine linear/circular depolarization measurements were performed during the nearest Aeolus overpass from the site on Friday evenings, with the same pointing geometry as Aeolus in order to reproduce the Aeolus measurements from the ground ( $35^\circ$  off-nadir from space corresponds to  $37.6^\circ$  off-zenith from ground, accounting also for the Earth's surface curvature). In total, 14 collocated eVe-Aeolus measurements were collected for the validation of the Aeolus Level 2A products. Additionally, targeted eVe measurements were performed during overflights from experimental aircraft carrying in situ and remote sensing instrumentation in the framework of the other JATAC components (CAVA-AW, CADDIWA, AVATART, and CPEX-CV) for synergistic studies. Finally, the eVe dataset contains lidar measurements implementing the dual-field-of-view (dual-FOV) technique [8] for evaluating the multiple scattering effects on lidar signals under cloudy and dusty conditions.

For the dual-FOV measurements, the configuration of the eVe lidar was modified from its routine configuration (i.e., linear and circular depolarization measurements) to a dual-FOV configuration. In the dual-FOV configuration, the two lasers were emitting linearly polarized light, and the two telescopes were equipped with a linear polarization analyzer in the detection unit while implementing different FOVs, i.e., a FOV of 2.4 mrad for telescope 1 and a FOV of 3.2 mrad for telescope 2.

### 3. Results

#### 3.1. Linear and Circular Depolarization Measurements

eVe measurements were used in a lidar intercomparison study between the eVe and PollyXT lidars in order to cross-validate both lidars and evaluate their performance [9]. For this comparison, the system was pointing at 5° off-zenith, the same as the pointing angle of the PollyXT systems. According to the intercomparison study, a very good agreement was observed between the retrieved aerosol optical properties profiles at 355 nm from eVe and PollyXT, with the observed discrepancies being related to the different signal-to-noise ratio (SNR) levels for the two systems. The intercomparison also revealed the capabilities of eVe to provide high-resolution products due to the low SNR of the system.

Targeted linear/circular depolarization measurements have been performed during the Aeolus overpass from the ASKOS site under multiple aerosol conditions, such as pure dust, marine and dust mixtures, and volcanic mixtures with marine and dust aerosols. For these measurements, eVe was pointing at 37.6° off-zenith towards the Aeolus track in order to reproduce the Aeolus measurements from the ground. Here, the Aeolus overpass on Friday 17 June 2022 was selected to demonstrate the retrieved eVe lidar products. The retrievals are obtained inside a mostly cloud-free time window (20:30 to 20:56 UTC), where further cloud screening has been applied to obtain cloud-free profiles. In the quicklook plots of Figure 1, we see that the Planetary Boundary Layer (PBL) extends up to 0.5 km and contains marine aerosols and depolarizing particles, which can be either dust particles or dehumidified marine aerosols [10]. Moreover, passing low clouds have formed at the top of PBL. On top of the PBL, at altitudes between 0.6 and 2 km, we observe several layers with moderate depolarization values, indicating the presence of a mixture of dust and marine aerosol or dehumidified marine aerosols [10]. Between 2 and 5 km, we observe a geometrically thick aerosol layer that, in some parts, has a lower concentration and consists mainly of dust and dust-dominated aerosol mixtures.

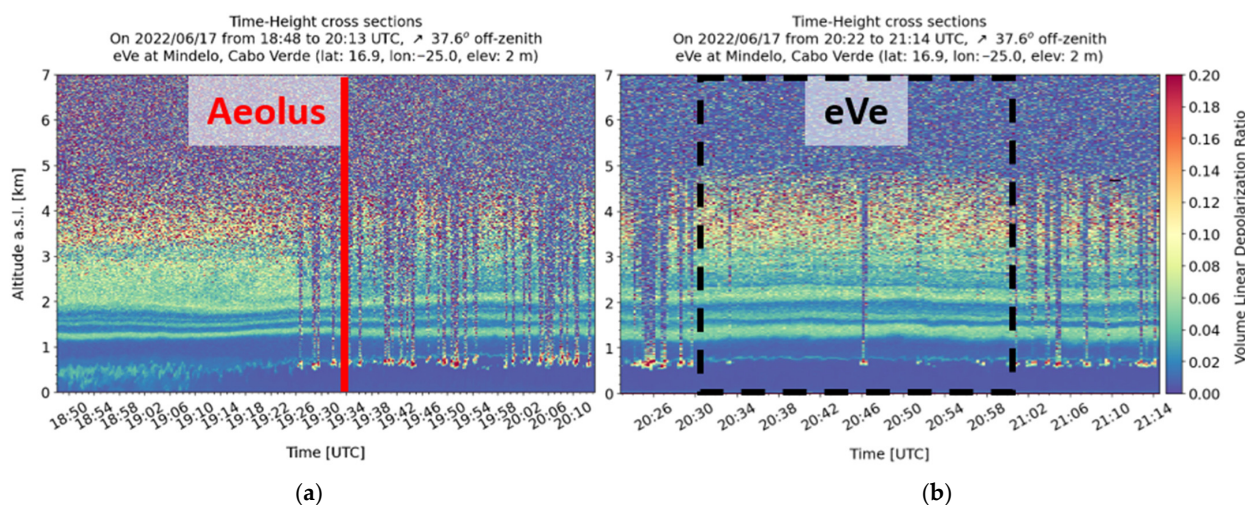


**Figure 1.** Time-height plot (quicklook) of the volume linear depolarization ratio from the daytime (a) and nighttime (b) eVe measurements during the Aeolus overpass (solid red line) on 17 June 2022 with pointing geometry of 37.6° off-zenith (↗). The dashed black rectangle denotes the mostly cloud-free time period selected for the retrieval of the eVe lidar products where additional cloud screening has been applied.

According to the averaged eVe profiles in Figure 2, inside the marine PBL (up to 0.5 km), the backscatter coefficient reaches up to  $8 \text{ Mm}^{-1} \text{ sr}^{-1}$ , the lidar ratio is around  $\sim 15 \text{ sr}$ , and the particle linear and circular depolarization ratios are close to zero. The depolarizing layers that top the PBL and extend up to 5.5 km have backscatter coefficient values that reach up to  $3.8 \text{ Mm}^{-1} \text{ sr}^{-1}$  and consist of marine and dust mixtures in the lower heights (0.6 to 2 km) and of a dust dominant layer from 2 to 5.5 km. For the depolarizing dust layers, the lidar ratio is close to  $51 \pm 11 \text{ sr}$ , and the particle linear and circular depolarization ratios range approximately from 0.15 to 0.25 and from 0.4 to 0.76, respectively. Moreover, at the altitude ranges where the depolarizing dust particles reside (1–5.5 km), the calculated Aeolus-like backscatter profile, which accounts only the co-polarized component of the backscattered signal (Appendix A of [7]), ranges from 0.4 to  $2 \text{ Mm}^{-1} \text{ sr}^{-1}$ , and it is underestimated with respect to the total backscatter profile by up to 47%. Similarly, the Aeolus-like lidar ratio is around 90 sr instead of the total lidar ratio of 51 sr, which results in an expected overestimation of approximately 76%.

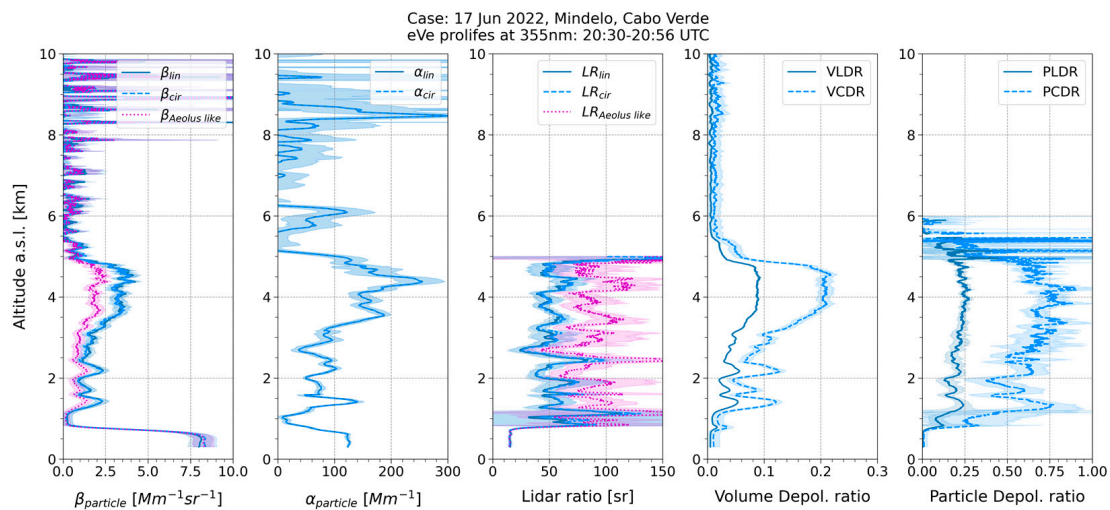


**Figure 2.** The eVe lidar products of particle backscatter ( $\beta_{\text{particle}}$ ) and extinction ( $\alpha_{\text{particle}}$ ) coefficients, lidar ratio, volume depolarization ratios, and particle depolarization ratios at 355 nm from linear (solid; dark blue) and circular (dashed; blue) emission, during the nearest Aeolus overpass from site on 17 June 2022. The Aeolus-like profiles (dotted; purple) have been calculated using the circular polarization profiles.

The eVe profiles of the extinction coefficient, the Aeolus-like backscatter coefficient, and the Aeolus-like lidar ratio are used as references in the comparison with the corresponding L2A profiles from Aeolus for the 14 overpasses during ASKOS (comparison plots not shown here). The Aeolus L2A profiles were obtained from the operational Aeolus baseline at that time. Overall, we found better agreement between Aeolus and eVe for the backscatter and extinction coefficients above 2.5 km, where the mean biases reach up to  $0.9 \text{ Mm}^{-1} \text{ sr}^{-1}$  and  $34 \text{ Mm}^{-1}$ , respectively. Below 2.5 km, the larger discrepancies can be attributed to the cloud contamination of the Aeolus profiles and the spatial inhomogeneity of the PBL (the minimum distance between the eVe location and the nearest Aeolus overpasses spans from 2 to 40 km over the ASKOS time). For the lidar ratio, larger discrepancies can be found in all heights, with a mean bias up to 290 sr in the dust layer heights due to the noisier lidar ratio profiles obtained from Aeolus.

### 3.2. Dual-Field-of-View Measurements

On 22 September 2022, nighttime dual-FOV measurements were performed from 04:38 to 06:11 UTC in the presence of a cloud located approximately 5 km away. According to the range-corrected signal and volume linear depolarization ratio quicklooks (Figure 3), the marine PBL extends up to  $\sim 1 \text{ km}$  also containing depolarizing particles of low concentration

around 0.8 km. The depolarizing particles are also suspended above the PBL and up to the cloud base at 5 km, forming dust and marine mixture layers.

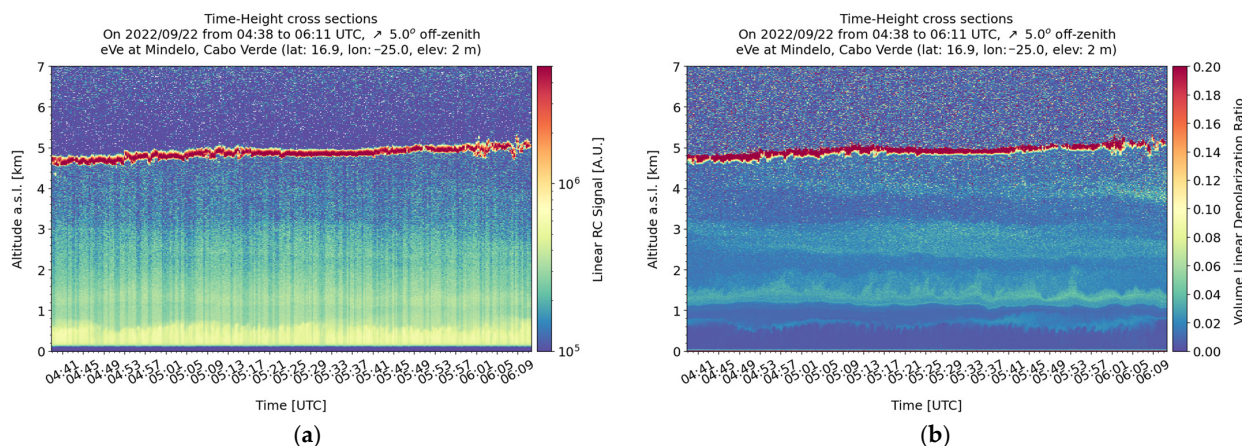


**Figure 3.** Time-height plot (quicklook) of the range-corrected lidar signal (a) and the volume linear depolarization ratio (b) from the dual-FOV measurement on 22 September 2022 with pointing geometry of 5° off-zenith (↗).

Figure 4 shows the comparison of the two VLDR profiles that are retrieved using the signals from the two telescopes with different FOVs. According to Figure 4, no deviations are observed below 4 km where the aerosols are present. However, at the height ranges where the cloud is located (4.5–5.5 km), the VLDR calculated from the signals collected from the telescope with the broader FOV (dashed red line) presents larger values than the VLDR calculated from the signals collected from the telescope with the narrower FOV (solid blue line). This deviation indicates the effect of the multiple scattering of the lidar beam inside the dense cloud on the recorded lidar signals and as an extension to the retrieved VLDR profiles, as expected under such conditions [11–13]. More dual-FOV measurements have been performed during clear days and heavy dust events. The clear days can be considered background cases since no deviations have been observed. For the dust cases, deviations are also observed, but not in the same order of magnitude as in the cloud cases.

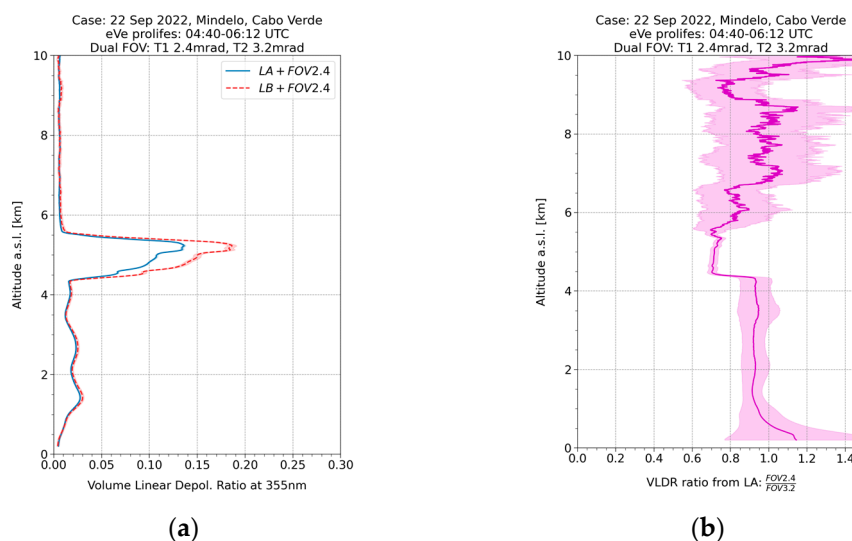


**Figure 4.** (a) Volume linear depolarization ratio (VLDR) profiles as retrieved using the lidar signals collected from telescope 1 (solid; blue) with the narrower FOV (2.4 mrad) and the lidar signals from telescope 2 (dashed; red) with the broader FOV (3.2 mrad) on 22 September 2022 from 04:40 to 06:12 UTC. (b) The calculated ratio of the two VLDRs as a function of altitude (solid; purple).

#### 4. Discussion/Conclusions

The eVe lidar, a combined linear/circular depolarization lidar and the ESA's ground reference system, was deployed in the ASKOS/JATAC campaign in 2021 and 2022. The acquired eVe dataset during the ASKOS operations has been used (a) against the PollyXT lidar measurements to cross-validate both lidars and evaluate their performance; (b) against Aeolus overpasses to provide reference measurements of the aerosol optical properties for the validation of the Aeolus L2A products; and (c) to investigate the multiple scattering effects of dust and cloud layers on lidar signals. The comparison between eVe and the Aeolus for the 14 collected overpasses revealed better agreement for the backscatter and extinction coefficients above 2.5 km but large discrepancies for the noisy Aeolus lidar ratio in all heights, while the cloud contamination on Aeolus profiles seems to increase the discrepancies below 2.5 km. The eVe dual-FOV measurements on clouds show deviations between the lidar products from the two different FOVs, revealing the effect of multiple scattering on the recorded lidar signals. Similar behavior is also observed inside dense dust layers, but the effect is considerably smaller. Nevertheless, further investigation should be performed for the observed deviations inside the dense dust layer.

**Author Contributions:** Conceptualization, P.P., E.M. and V.A.; methodology, P.P., N.S., E.M. and V.A.; software, P.P. and N.S.; formal analysis, P.P.; investigation, P.P., N.S. and E.M.; data curation, P.P., N.S., S.M.I., D.T.Q. and D.D.F.A.; writing—original draft preparation, P.P.; writing—review and editing, E.M. and C.M.; visualization, P.P.; supervision, C.M. and V.A.; project administration, V.A., E.M., J.v.B. and T.F. All authors have read and agreed to the published version of the manuscript.

**Funding:** This research was financially supported by the PANGAEA4CalVal project (Grant Agreement 101079201) funded by the European Union, and the European Space Agency's project of ASKOS (Grant agreement 4000131861/20/NL/IA).

**Institutional Review Board Statement:** Not applicable.

**Informed Consent Statement:** Not applicable.

**Data Availability Statement:** The acquired eVe measurements during the ASKOS operations are available under an SFTP server with host name: [askos.space.noa.gr](https://askos.space.noa.gr). You can contact the main author for more details. The complete ASKOS and JATAC dataset will soon be available in [evdc.esa.int](https://evdc.esa.int).

**Acknowledgments:** We acknowledge the support of Raymetrics S.A. on the operation of the eVe lidar for the ASKOS needs in Cabo Verde.

**Conflicts of Interest:** The authors declare no conflict of interest.

#### References

1. Stoffelen, A.; Pailleux, J.; Källén, E.; Vaughan, J.M.; Isaksen, L.; Flamant, P.; Wergen, W.; Andersson, E.; Schyberg, H.; Culoma, A.; et al. The atmospheric dynamics mission for global wind field measurement. *Bull. Am. Meteorol. Soc.* **2005**, *86*, 73–88. [[CrossRef](#)]
2. Reitebuch, O. *The Spaceborne Wind Lidar Mission ADM-Aeolus*; Schumann, U., Ed.; Springer: Berlin/Heidelberg, Germany, 2012; pp. 815–827. [[CrossRef](#)]
3. Tan, D.G.; Andersson, E.; Kloe, J.D.; Marseille, G.J.; Stoffelen, A.; Poli, P.; Denneulin, M.L.; Dabas, A.; Huber, D.; Reitebuch, O.; et al. The ADM-Aeolus wind retrieval algorithms. *Tellus A Dyn. Meteorol. Oceanogr.* **2008**, *60*, 191–205. [[CrossRef](#)]
4. Flament, T.; Tracon, D.; Lacour, A.; Dabas, A.; Ehlers, F.; Huber, D. Aeolus L2A aerosol optical properties product: Standard correct algorithm and Mie correct algorithm. *Atmos. Meas. Tech.* **2021**, *14*, 7851–7871. [[CrossRef](#)]
5. Fehr, T.; McCarthy, W.; Amiridis, V.; Baars, H.; von Bismarck, J.; Borne, M.; Chen, S.; Flamant, C.; Marenco, F.; Knipperz, P.; et al. The Joint Aeolus Tropical Atlantic Campaign 2021/2022 Overview—Atmospheric Science and Satellite Validation in the Tropics. In Proceedings of the EGU General Assembly 2023, Vienna, Austria, 24–28 April 2023. EGU23-7249. [[CrossRef](#)]
6. Marinou, E.; Amiridis, V.; Paschou, P.; Tsikoudi, I.; Tsekeri, A.; Daskalopoulou, V.; Baars, H.; Floutsi, A.; Kouklaki, D.; Pirloaga, R.; et al. ASKOS Campaign 2021/2022: Overview of measurements and applications. In Proceedings of the EGU General Assembly 2023, Vienna, Austria, 24–28 April 2023. EGU23-16530. [[CrossRef](#)]
7. Paschou, P.; Siomos, N.; Tsekeri, A.; Louridas, A.; Georgoussis, G.; Freudenthaler, V.; Biniotoglou, I.; Tsaknakis, G.; Tavernarakis, A.; Evangelatos, C.; et al. The eVe reference polarisation lidar system for the calibration and validation of the Aeolus L2A product. *Atmos. Meas. Tech.* **2022**, *15*, 2299–2323. [[CrossRef](#)]

8. Jimenez, C.; Ansmann, A.; Engelmann, R.; Donovan, D.; Malinka, A.; Seifert, P.; Wiesen, R.; Radenz, M.; Yin, Z.; Bühl, J.; et al. The dual-field-of-view polarization lidar technique: A new concept in monitoring aerosol effects in liquid-water clouds—Theoretical framework. *Atmos. Chem. Phys.* **2020**, *20*, 15247–15263. [[CrossRef](#)]
9. Paschou, P.; Siomos, N.; Marinou, E.; Baars, H.; Gkikas, A.; Georgoussis, G.; Althausen, D.; Engelmann, R.; von Bismarck, J.; Fehr, T.; et al. First Results from the Aeolus reference lidar eVe during the tropical campaign JATAC at Cabo Verde. In Proceedings of the 30th International Laser Radar Conference, 26 June–1 July 2022.
10. Haarig, M.; Ansmann, A.; Gasteiger, J.; Kandler, K.; Althausen, D.; Baars, H.; Radenz, M.; Farrell, D.A. Dry versus wet marine particle optical properties: RH dependence of depolarization ratio, backscatter, and extinction from multiwavelength lidar measurements during SALTRACE. *Atmos. Chem. Phys.* **2017**, *17*, 14199–14217. [[CrossRef](#)]
11. Bissonnette, L.R.; Brusaglioni, P.; Ismaelli, A.; Zaccanti, G.; Cohen, A.; Benayahu, Y.; Kleiman, M.; Egert, S.; Flesia, C.; Schwendemann, P.; et al. LIDAR multiple scattering from clouds. *Appl. Phys. B Laser Opt.* **1995**, *60*, 355–362. [[CrossRef](#)]
12. Donovan, D.P.; Klein Baltink, H.; Henzing, J.S.; De Roode, S.R.; Siebesma, A.P. A depolarisation lidar-based method for the determination of liquid-cloud microphysical properties. *Atmos. Meas. Tech.* **2015**, *8*, 237–266. [[CrossRef](#)]
13. Jimenez, C.; Ansmann, A.; Engelmann, R.; Donovan, D.; Malinka, A.; Seifert, P.; Wiesen, R.; Radenz, M.; Yin, Z.; Bühl, J.; et al. The dual-field-of-view polarization lidar technique: A new concept in monitoring aerosol effects in liquid-water clouds—case studies. *Atmos. Chem. Phys.* **2020**, *20*, 15265–15284. [[CrossRef](#)]

**Disclaimer/Publisher’s Note:** The statements, opinions and data contained in all publications are solely those of the individual author(s) and contributor(s) and not of MDPI and/or the editor(s). MDPI and/or the editor(s) disclaim responsibility for any injury to people or property resulting from any ideas, methods, instructions or products referred to in the content.